

# Structure and Dynamics of a Poly(dimethylsiloxane) Network: A Comparative Investigation of Gel and Solution

Anne-Marie Hecht,<sup>†</sup> Armel Guillermo,<sup>†</sup> Ferenc Horkay,<sup>‡</sup> Simon Mallam,<sup>†,§</sup> Jean François Legrand,<sup>||</sup> and Erik Geissler<sup>\*,†</sup>

Laboratoire de Spectrométrie Physique,<sup>⊥</sup> Université Joseph Fourier de Grenoble, B.P. 87, 38402 St. Martin d'Hères Cedex, France, Department of Colloid Science, Loránd Eötvös University, H-1117 Budapest, Pázmány Péter sétány 2, Hungary, and Institut Laue-Langevin, 156X Centre de Tri, 38042 Grenoble Cedex, France

Received December 11, 1991; Revised Manuscript Received April 2, 1992

**ABSTRACT:** Combined measurements are described involving elastic and quasi-elastic neutron scattering, quasi-elastic light scattering, nuclear magnetic resonance, and swelling pressure on an end-linked poly-(dimethylsiloxane) (PDMS) gel swollen to equilibrium in a good solvent (toluene) and the equivalent solution. The factors affecting the collective diffusion coefficient are considered. The swelling pressure measurements show that the osmotic modulus is appreciably depressed in the gel. The neutron spin-echo measurements reveal no difference in the dynamic response at intermediate and high values of the scattering vector  $Q$ . Elastic neutron scattering at small  $Q$  detects nonuniformities in the network structure, which are absent from the solution. These nonuniformities play a major role in the dynamic response of the system at lower  $Q$  and appear to be the cause of the observed reduction in osmotic pressure. The NMR measurements show a small increase of the solvent mobility in the gel, which is consistent with the appearance of structural nonuniformities in the system.

## Introduction

In classical theories of network swelling<sup>1,2</sup> it is assumed that the only distinction between polymer solutions and gels is the existence of a permanent elastic shear modulus  $G$  in the network. The free energy of the gel is expressed as the sum of an elastic contribution and a free energy of mixing. In scaling approaches the analogy between the mixing free energy of the gel and that of the solution is maintained.<sup>3</sup> Measurements of solvent vapor pressure over polymer solutions and the equivalent gel<sup>4-7</sup> have, however, revealed significant differences between the thermodynamic properties of the two states. Such discrepancies can be interpreted either as anomalies in the network elastic free energy<sup>6,7</sup> or as a change in the osmotic mixing interaction between the solution and the gel.<sup>8-10</sup> Evidence from macroscopic experiments is more consistent with a lower osmotic pressure in the gel, but the associated change in the polymer-solvent interaction parameter is not, as sometimes proposed,<sup>8,10</sup> simply proportional to the number of cross-linking points: the decrease in osmotic pressure is found to be almost independent of the cross-linking density of the gel.<sup>11,12</sup> The underlying cause of the difference is not yet satisfactorily explained.

The microscopic behavior of swollen polymer networks may be expected to be sensitive to thermodynamic changes in the system. For solutions, the collective diffusion coefficient  $D_c$  gives a measure of the hydrodynamic correlation length  $\xi_H$ .

$$D_c = K_{os}/f \quad (1)$$

where  $K_{os} (= \varphi \partial \Pi / \partial \varphi)$ ,  $\Pi$  being the osmotic pressure) is the osmotic modulus.  $f$  is the polymer-solvent friction coefficient

$$f = 6\pi\eta/\xi_H^2 \quad (2)$$

where  $\eta$  is the viscosity of the solvent. In a gel, on account

of the elastic modulus  $G$ , eq 2 transforms to<sup>13</sup>

$$D_c = M_{os}/f \quad (3)$$

where  $M_{os}$  is the longitudinal osmotic modulus.

Several authors<sup>14-17</sup> have observed quasi-elastic light scattering measurements in which  $D_c$  is larger in the gel than in solution. The opposite result has, however, also recently been reported.<sup>18</sup>

Further microscopic information is provided by small-angle scattering of neutrons or X-rays, which yields the static correlation length  $\xi_s$ . Generally the spectra from neutral solutions at polymer volume fraction  $\varphi$  adopt an Ornstein-Zernicke (Lorentzian) form

$$I(Q) = a \frac{(d_p - d_s)^2 k T \varphi^2}{K_{os}} \frac{1}{1 + Q^2 \xi_s^2} \quad (4)$$

where  $a$  is an apparatus constant,  $d_p$  and  $d_s$  are respectively the scattering densities of the polymer and solvent for neutrons or X-rays, and  $k$  and  $T$  are the Boltzmann constant and the absolute temperature.  $Q = [4\pi/\lambda] \sin(\theta/2)$  is the usual scattering vector,  $\theta$  being the scattering angle and  $\lambda$  the incident wavelength. In eq 4 it is supposed that  $Q\xi_s \leq 1$ .

For gels, the scattering response is more complex than eq 4 because the distribution of cross-links is not in general uniform: where these are densely clustered, the network is gathered into regions of higher concentration, while less cross-linked areas are looser and swell more. Such permanent departures from uniformity participate little in the dynamic fluctuations. It has been shown recently in several gel systems<sup>19-23</sup> that the scattering pattern from these static accumulations of polymer can be subtracted out of the SANS or SAXS spectra to reveal a liquidlike spectrum similar to eq 4. The values of  $\xi_s$  deduced for the gel are generally larger than those in the solution of the same mean concentration.

Two possible explanations arise for the difference in osmotic behavior between the gel and the solution. The first is that the constraints due to cross-links modify the statistical arrangement within a polymer chain: this implies changes in the mobility of the polymer chains.

<sup>†</sup> Université Joseph Fourier de Grenoble.

<sup>‡</sup> Loránd Eötvös University.

<sup>§</sup> Present address: Centre for Energy Research and Training, Ahmadu Bello University, Zaria, Nigeria.

<sup>||</sup> Institut Laue-Langevin.

<sup>⊥</sup> CNRS associate laboratory.

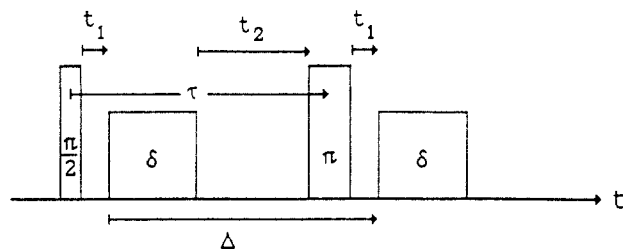


**Figure 1.** Field gradient pulse sequence for measurement of translational diffusion coefficient  $D_T$  of toluene in PDMS. Radio-frequency pulses are designated by  $\pi/2$  and  $\pi$ , and field gradient pulses are of length  $\delta$ .

The second explanation is that the large-scale nonuniformities of concentration in the gel alter the values of the average observed quantities.

The purpose of this paper is to investigate the different factors contributing to  $D_c$  by making comparative measurements between a gel and a solution, using a range of different experimental techniques. To this end, we describe thermodynamic and mechanical observations on a poly(dimethylsiloxane) gel fully swollen in toluene and on the equivalent solution. The static scattering properties of these samples, investigated by SANS, are compared with the results of osmotic investigations. The dynamic response of the polymer was measured by quasi-elastic light scattering at small  $Q$  and also by neutron spin echo to explore the movement of the polymer chains at larger  $Q$  vectors. The solvent mobility was probed by nuclear magnetic resonance.

## Experimental Procedures

**Sample Preparation.** As reported elsewhere,<sup>19,22,24</sup> the gels were prepared from a melt of  $\alpha,\omega$ -dihydroxy-terminated PDMS chains, kindly supplied by Dr. P. Pruvost of Département Silicones, Rhône-Poulenc, France. The viscosity-average molecular weight of the precursor chains was  $M_v = 40\,000$ . The cross-linking agent, ethyltriacetoxysilane (ETAS) was mixed in a dry-nitrogen atmosphere to produce a precursor mixture that develops cross-links when exposed to atmospheric water. No catalyst was added. The mixture was poured into a PTFE mold and left for 2 months in a dust-free box in contact with the atmosphere.

At the end of the curing process, the samples were stripped from their molds and washed in octane, and the diluent was replaced by toluene, which is also a good solvent for PDMS at 25 °C. The extractable material, removed by successive solvent exchanges, did not exceed 4–5% by weight. The swelling equilibrium concentration of the samples in excess toluene was measured.

The PDMS solution was prepared at the same concentration as the fully swollen gel from the same batch of PDMS, in the absence of a cross-linking agent.

**Swelling Pressure.** The swelling pressure was measured by enclosing the gels in dialysis bags and allowing them to come to equilibrium with a solution of poly(vinyl acetate) in toluene of known osmotic pressure.<sup>25,26</sup> After reaching equilibrium (1–4 weeks, depending on sample size), the concentration of both the solution and the gel was measured. The swelling pressure of the PDMS gels was calculated from the osmotic pressure of the equilibrium polymer solution. At each concentration the shear modulus was measured.<sup>24</sup> The polymer volume fractions were calculated from the known densities at 25 °C of PDMS<sup>27</sup> ( $\rho_{\text{PDMS}} = 0.97 \text{ g cm}^{-3}$ ) and protonated toluene ( $\rho_{\text{ToH}} = 0.861 \text{ g cm}^{-3}$ ),<sup>8</sup> using the assumption of volume additivity.

**Nuclear Magnetic Resonance.** NMR measurements were performed at 36 MHz using a  $\pi/2$ – $\tau$ – $\pi$  sequence in which a pulsed field gradient  $g$  is applied to the sample for a time  $\delta$  following each of the  $\pi/2$  and  $\pi$  radio-frequency pulses according to the scheme shown in Figure 1.<sup>28</sup> At time  $2\tau$  the field gradient

attenuates the echo amplitude in the ratio

$$E(g)/E(g=0) = \exp(-\gamma^2 D_T X)$$

where

$$X = g^2 \delta^2 (\Delta - \delta/3) - \delta g g_0 [t_1^2 + t_2^2 + \delta(t_1 + t_2) + 2\delta^2/3 - 2\tau^2] \quad (5)$$

and in the present case

$$\tau = t_1 + \delta + t_2 \quad \text{and} \quad \Delta = \tau$$

$\Delta$  being the interval between the leading edges of the field gradient pulses (Figure 1). The NMR Larmor angular frequency is  $\omega_0 = \gamma H_0$ ,  $g_0$  is the gradient of the steady magnetic field  $H_0$ , and the gyromagnetic ratio  $\gamma$  for protons is  $26\,752 \text{ s}^{-1} \text{ G}^{-1}$ . Calibration of the field gradients  $g$  and  $g_0$  was performed by comparison with the diffusion coefficient of  $\text{H}_2\text{O}$ .<sup>29</sup> By means of this calibration and eq 5, a value of  $D_T$  for toluene was obtained,  $(2.3 \pm 0.1) \times 10^{-5} \text{ cm}^2 \text{ s}^{-1}$ , in good agreement with the results of Vrentas et al.<sup>30</sup> To measure the translation diffusion coefficient  $D_T$  in the solution and in the gel, protonated toluene was used as diluent. On account of the low polymer concentration, the signal from the poly(dimethylsiloxane) is much smaller than that of the diluent. The two signals are easily distinguished because residual dipolar interactions between protons on the polymer chains make their transverse relaxation time  $T_2$  much shorter than that of the toluene, with the result that only the solvent signal survives at long times. Nonetheless, measurements were also made of  $D_T$  in poly(dimethylsiloxane) in deuterated toluene, where the only contribution to the signal comes from the polymer. In this case the echo attenuation was not a simple exponential, probably because of polydispersity in the sample. A stretched exponential of the form  $\exp[-(\gamma^2 D_T X)^s]$  with  $s = 0.75$  yielded a good approximation for the decay function.

**Quasi-Elastic and Static Neutron Scattering.** Neutron spin echo is now a well-established technique that is especially suited for probing the dynamic properties of polymer systems at values of  $Q$  greater than are attainable by light scattering, when high resolution is required.<sup>31–33</sup> The procedure measures the loss of phase coherence in polarized neutrons as they are scattered inelastically by movements in the sample. Although the phase of the neutron polarization is coherent, the total wave function of the neutron beam has no coherence, so that heterodyning and its associated uncertainties can be discounted. The procedure consists of polarizing the incident beam parallel to the direction of flight and then rotating the neutron spins by  $\pi/2$  with an off-axis magnetic pulse. After traveling a fixed distance through a steady precession field  $H$ , the neutrons are then subjected to a  $\pi$  pulse just before being scattered by the sample. After the sample, a  $(-H)$ ,  $\pi/2$  sequence is applied, and the residual magnetic moment is measured by a polarization analyzer. The loss of intensity in the measured spin echo results from changes in the velocity distribution of the neutrons produced by inelastic scattering in the sample. By varying the magnetic field  $H$ , different precession angles of the spins are explored, in a way that is equivalent to varying the time separation between radio-frequency pulses in a conventional pulsed NMR experiment.

The measurements were made on the IN11 instrument at the Institut Laue-Langevin (ILL), Grenoble, France, at three incident wavelengths: 5.7, 8.7, and 11.3 Å, with a wavelength spread  $\Delta\lambda/\lambda$  of about 20%. These wavelengths span the time delay windows 0–5, 0–16, and 0–37 ns, respectively. The total  $Q$  range explored was between 0.025 and 0.477 Å<sup>−1</sup>. At the highest  $Q$  value the signal decay was too fast to give meaningful results. The object of the 11.3-Å measurements was to extend the observations on the gels to longer delay times.

The samples were contained in rectangular niobium cells of inner dimensions 4 × 30 × 40 mm<sup>3</sup>, and the gel was cut so that it just filled this space when fully swollen in toluene. A circular cadmium diaphragm of diameter 25 mm was fixed to the sample holder to limit the effective area of the beam. Fully deuterated toluene was used as the diluent for both network and solution, the latter being prepared to have the same concentration as the fully swollen gel ( $\varphi = 0.129$ ).

Static SANS measurements were also made on the D11 instrument at ILL. The 64 × 64 cell detector was placed at distances between 1.2 and 4 m from the sample, with an incident

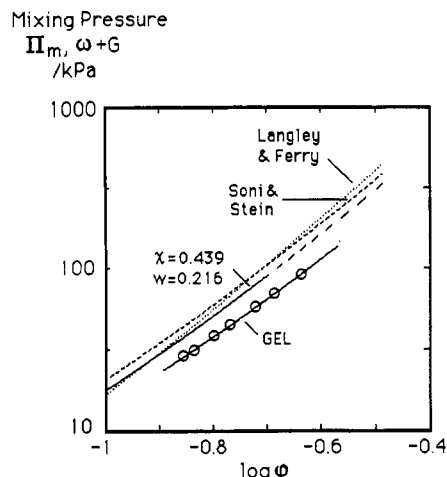


**Figure 2.** Mixing pressure of the gel (circles) and the solution (lines) calculated from refs 8, 19, and 35. A continuous line through gel points is given by eq 7 with  $\chi = 0.443$  and  $w = 0.332$ .

wavelength of 6 Å, yielding an effective range in  $Q$  between 0.012 and 0.25 Å<sup>-1</sup>. The samples were contained between quartz windows separated by an annular Teflon spacer of thickness 2 mm. Exposure times varying between 20 min and 1 h were used, depending on the sample-detector distance.

**Quasi-Elastic Light Scattering.** Quasi-elastic light scattering measurements were made using a He-Ne laser with a fixed scattering angle of 39°, the output of the photomultiplier being analyzed by a single-bit digital correlator. The samples were held in scattering cells with quartz windows separated by a 4-mm Teflon ring spacer, chosen so that the gel could swell fully to equilibrium in the available space. The same holder housed the solution, and the sample position was adjusted by a micrometer screw to select regions of the entrance window giving sufficient flare to introduce an appropriate local oscillator field. For the gel, static heterogeneities within the network scattered light sufficiently strongly to ensure heterodyning.

For the solution, displacement of the observation zone in the sample from close to a window to the cell center caused the observed decay rate to increase by a factor of 2, as may be expected when the detection mode is changed from heterodyne to homodyne. Measurements were made at room temperature (20 °C) and corrected to 26.5 °C through the known temperature variation of the solvent viscosity in eq 1.

## Results

**Swelling Pressure.** The osmotic pressure of a polymer solution can usually be described satisfactorily by the Flory-Huggins formalism<sup>2</sup>

$$\Pi = -(RT/v_1)[\ln(1-\phi) + \phi(1-1/x) + \chi\phi^2 + w\phi^3] \quad (6)$$

where  $R$  is the gas constant,  $v_1$  is the molar volume of the solvent,  $x$  is the ratio of the molar volume of the polymer to that of the solvent, and  $\chi$  and  $w$  are respectively the second- and third-order interaction parameters.

In a network in equilibrium with a pure solvent, the osmotic pressure of the chains,  $\Pi_{mg}$ , is equal to the elastic restoring pressure of the polymer coils.<sup>34</sup> In simple networks not subject to local association effects such as crystallization or hydrogen bonding, the elastic restoring pressure is equal to the elastic modulus,  $G$ . (The subscript  $m$  in  $\Pi_{mg}$  denotes "mixing", i.e., the osmotic pressure of a polymer of infinite molecular weight.) The pressure exerted during swelling is thus

$$\omega = \Pi_{mg} - G \quad (7)$$

The mixing pressure of the gel,  $\Pi_{mg}$ , is obtained from the swelling pressure  $\omega$  and the shear modulus  $G$ , both of which are directly measured quantities. In Figure 2 the quantity  $\Pi_{mg} = \omega + G$  is shown as a function of

**Table I**  
Interaction Parameters for PDMS-Toluene Solutions at  $T = 25$  °C Obtained from Equation 7

sample	$\chi$	$w$	ref
solution	0.465	0	8 and 27
solution	0.430	0.179	35
solution	0.439	0.216	19 and this work
gel	0.443	0.332	

concentration for the gel investigated here (open circles) at 25 °C. Also shown are various estimates of the mixing pressure  $\Pi_m$  (i.e.,  $x = \infty$ ), for PDMS-toluene solutions at the same temperature. The curves of  $\Pi_m$  vs  $\phi$  displayed are literature data,<sup>8,19,27,35</sup> obtained by various different techniques (swelling measurements, static light scattering, and SANS), and are all in plausible mutual agreement. The data for the gel lie significantly below the solution curves. Table I lists the parameters, found for PDMS toluene solutions by the different authors, in the expression for the mixing pressures

$$\Pi_m = -(RT/v_1)[\ln(1-\phi) + \phi + \chi\phi^2 + w\phi^3] \quad (8)$$

Application of eq 8 to the mixing pressure of the gel,  $\Pi_{mg} = \omega + G$ , yields  $\chi = 0.443$  and  $w = 0.331$  and is displayed in Figure 2 (continuous line through experimental points).

According to eq 4, the scattering intensity from a polymer solution is inversely proportional to the osmotic compressional modulus  $K_{os}$ . For polymer solutions of high molecular weight ( $x \rightarrow \infty$ ), eq 8 gives for this quantity

$$K_{os} = \phi(\partial\Pi_m/\partial\phi) = (RT/v_1)\phi^2[1/(1-\phi) - 2\chi - 3w\phi] \quad (9)$$

Thus, for a solution at the same concentration as the swollen PDMS network investigated here ( $\phi = 0.129$ ), eq 9 yields

$$\text{Solution: } K_{os} = 71.9 \text{ kPa} \quad (9a)$$

(using  $\chi = 0.439$  and  $w = 0.216$ ). The equivalent calculation for the gel ( $\chi = 0.443$ ,  $w = 0.331$ ) gives

$$\text{Gel: } K_{os} = \phi(\partial\Pi_{mg}/\partial\phi) = 51.9 \text{ kPa} \quad (9b)$$

In gels, the osmotic modulus governing the intensity of quasi-elastically scattered light or neutrons is the longitudinal osmotic modulus<sup>13</sup>

$$M_{os} = \phi\partial\omega/\partial\phi + 4G/3 \quad (10)$$

The elastic modulus of the gel obeys a relation of the form

$$G = G_0\phi^m \quad (11)$$

where the experimentally determined parameters are respectively  $G_0 = 54.9 \pm 0.4$  kPa and  $m = 0.330 \pm 0.004$  (Figure 3). This value of  $m$  is in agreement with the classical prediction  $m = 1/3$ .<sup>34</sup> Taking  $m = 1/3$  gives for  $M_{os}$  at equilibrium swelling concentration  $\phi_e$

$$M_{os} = 79.6 \text{ kPa} \quad (12)$$

The results in eqs 9a and 12 state that in scattering measurements on this gel the reduction of mixing pressure caused by cross-linking is overcompensated slightly (ca. 10%) by the contribution of the elastic modulus.

**Small-Angle Neutron Scattering.** The results of small-angle neutron elastic scattering measurements on PDMS gels and solutions have been described elsewhere.<sup>19</sup> The scheme used separated the scattering spectra of the swollen gels into a static part and a liquidlike part,  $I_s(Q)$  and  $I_L(Q)$ , each having a distinct characteristic length.

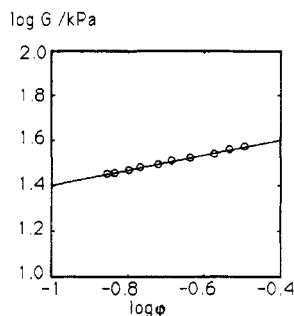


**Figure 3.** Measured values of the elastic shear modulus  $G$  as a function of swelling. The straight line shown has a slope  $m = 0.330$ .

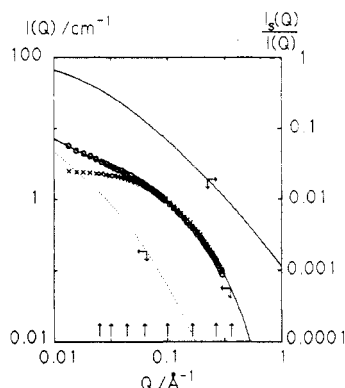


**Figure 4.** Double-logarithmic representation of the SANS signal from gel (O) and solution (X). The dotted line is the amplitude of the static component in the gel signal calculated from eqs 16 and 17. Right-hand curve: static intensity expressed as a fraction of the total scattering.  $Q$  vectors explored in the neutron spin-echo experiment are shown by vertical arrows on the ordinate axis.

$I_S(Q)$  is the intensity scattered by the permanent non-uniformities in the polymer concentration maintained by the cross-links, while the liquidlike (ergodic) part  $I_L(Q)$  arises from thermodynamic fluctuations of the polymer chains around these mean positions. In a SANS experiment the decomposition

$$I(Q) = I_S(Q) + I_L(Q) \quad (13)$$

is not unique. The choice of the form of the two components is limited by the condition of invariance;<sup>36</sup> i.e., in a statistically isotropic binary system that has no long-range order

$$\int_0^\infty I(Q) Q^2 dQ = a[2\pi^2(d_p - d_s)^2 \langle \Delta\phi^2 \rangle] \quad (14)$$

where

$$\begin{aligned} \langle \Delta\phi^2 \rangle &= \phi(1 - \phi) \\ &= \langle \Delta\phi^2 \rangle_S + \langle \Delta\phi^2 \rangle_L \end{aligned} \quad (15)$$

At small values of  $Q$ , the thermodynamic contribution  $I_L(Q)$  is approximated by expression 4. At short distances, however, the polymer chain behaves like a rod of finite radius  $r_c$ . This means that at large  $Q$  the scattering function tends to  $(1/Q) \exp(-Q^2 r_c^2/2)$ . Thus

$$I_L(Q) = A(1 + Qr_c/\sqrt{2}) \exp(-Q^2 r_c^2/2)/(1 + Q^2 \xi^2) \quad (16)$$

This form,<sup>20</sup> which possesses a finite second moment and agrees well with the observed shape of the scattering function for the solutions at high  $Q$  in the concentration range investigated here (cf. Figure 4), yields a value  $r_c \approx 4.0$  Å.

For the static scattering spectrum  $I_S(Q)$ , earlier observations on hydrogels<sup>37</sup> and recent work on randomly cross-

**Table II**  
Scattering Parameters for a Swollen PDMS Network and a Solution, Analyzed with Equations 16 and 17

	$\phi$	$A_{\text{calc}}/ \text{cm}^{-1}$	$A/ \text{cm}^{-1}$	$B/ \text{cm}^{-1}$	$\xi/ \text{\AA}$	$\langle \delta\phi^2 \rangle$
gel	0.166	2.69	2.44 <sup>a</sup>	0.0105 $Q^{-4/3}$	15.7 <sup>a</sup>	$2.4 \times 10^{-3}$
solution	0.155		2.45		14.5	

<sup>a</sup> The decomposition procedure of ref 19 for this sample yielded  $A = 3.43 \text{ cm}^{-1}$  and  $\xi = 16.7 \text{ \AA}$ . <sup>b</sup>  $A$  calculated from eqs 8 and 9 for the same gel sample as in ref 19 ( $G = 26.7 \text{ kPa}$ ).

**Table III**  
Translational Diffusion Coefficients from Field Gradient Proton NMR

sample	$\phi$	$T/^\circ\text{C}$	$D_T/10^5 \text{ cm}^2 \text{ s}^{-1}$
Tol H	0	26.5	$2.3 \pm 0.1$
Tol H	0	31.5	$2.45 \pm 0.1$
sol/Tol H	0.129	26.5	$1.86 \pm 0.07$
sol/Tol H	0.129	31.5	$1.96 \pm 0.07$
gel/Tol H	0.129	26.5	$1.98 \pm 0.09$
gel/Tol H	0.129	31.5	$2.16 \pm 0.08$
sol/Tol D	0.129	26.5	$0.0152 \pm 0.006^a$

<sup>a</sup> Obtained from a stretched exponential.

linked swollen networks<sup>38,39</sup> suggest that this contribution may be fractallike, with an intensity varying as  $Q^{-p}$  over a limited range. The requirement of a finite value for  $\langle \Delta\phi^2 \rangle_S$  implies a cutoff at high  $Q$  for such a distribution. A simple choice for the cutoff is the same as that adopted for  $I_L(Q)$ ; i.e.

$$I_S(Q) = BQ^{-p} \exp(-Q^2 r_c^2/2)/(1 + Q^2 \xi^2) \quad (17)$$

The representation of  $I_S(Q)$  by eq 17 is a convenient but not unique choice. Other simple expressions involving  $r_c$  and  $\xi$ , however, produce unphysical values for the coefficient  $B$  or else give notably poorer fits to the data. Equation 17 introduces only two new adjustable parameters ( $B$  and  $p$ ) in addition to those for the solution. [An objection to eq 17 is its  $Q \rightarrow 0$  behavior. Observation of the lower cutoff in the  $Q^{-p}$  behavior is masked by scattering from large poly(ethylsiloxane) particles that form during the cross-linking process,<sup>22</sup> but in the  $Q$  range of interest for the present neutron scattering measurements, the contribution from these particles is vanishingly small. The lower cutoff in the  $Q^{-p}$  behavior of the polymer spectrum is not in fact important for the calculation of the second moment (provided  $p < 3$ ), but ignorance of the low  $Q$  response of the system is a handicap in estimating the collective diffusion coefficient  $D_c$  (see below).]

The use of a stretched exponential form<sup>20</sup> in the place of eq 17 gives an acceptable alternative fit but requires an additional parameter. Other descriptions of the static structure factor of gels based on a purely fractal approach<sup>39</sup> do not fit our results at all.

Substitution of eqs 16 and 17 into eq 11 yields good fits to the spectra in the  $Q$  range explored (Figure 4). For a set of identical PDMS gels at different degrees of swelling, nonlinear least-squares fitting, in which the four parameters  $A$ ,  $B$ ,  $p$ , and  $\xi$  are allowed to vary, gives  $p \approx 4/3$  in each case. The value of  $p$  is therefore taken as fixed, thus leaving only three free variables. The resulting correlation lengths  $\xi$  are greater than those in the solution. Table II lists the parameters obtained from this analysis for a typical gel sample.

**Nuclear Magnetic Resonance.** The results of NMR measurements are listed in Table III. The translational diffusion coefficient of the solvent molecules may also be

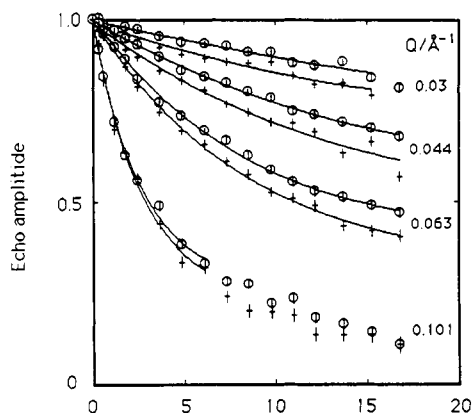


**Figure 5.** Neutron spin-echo amplitudes of the signal from PDMS-toluene gel (O) and solution (+) at incident wavelength  $\lambda = 8.7$  Å. Curves shown are two-cumulant fits to the data.

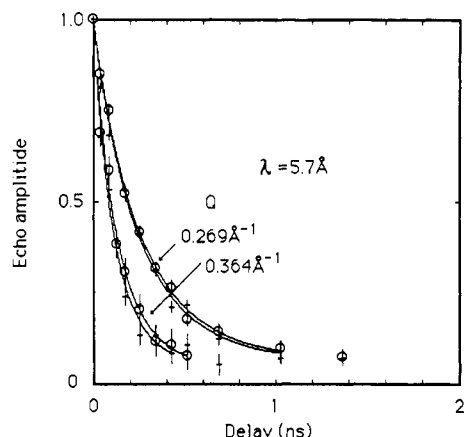


**Figure 6.** Neutron spin-echo amplitudes of the signal from PDMS-toluene gel (O) and solution (+) at incident wavelength  $\lambda = 5.7$  Å.

written in the Stokes-Einstein form

$$D_T = kT/(6\pi\eta a) \quad (18)$$

where  $a$  is an effective radius of a toluene molecule. Inspection of Table III reveals that the effective viscosities felt by the diluent in the gel and the solution are not greatly different, but their probable relative order is  $\eta_{\text{sol}} > \eta_{\text{gel}}$ . Such a change would be consistent with a change in the spatial arrangement of the polymer in the gel (see the Discussion).

**Neutron Spin Echo.** Typical spin-echo relaxation curves are shown in Figures 5 and 6 for the solution (+) and the swollen PDMS gel (O). These curves are corrected for solvent scattering and elastic scattering from the niobium container. Smaller apparent relaxation rates for the gel than for the solution can be seen in the lower  $Q$  range. Before interpreting these results, however, it is essential to identify possible sources of static scattering that may give rise to a constant background and increase the apparent time constant of the decay. In the case of polymer melts, a quasi-static component can arise due to the constraining presence of entanglements surrounding a given marked chain.<sup>40,41</sup> In the present gels, there are no marked chains, and the coherent scattering is associated only with the contrast between the polymer and solvent. The principal sources of static scattering in these samples are as follows:

(1) **Static Accumulations of Polymer.** In polymer solutions the concentration is smooth for distances greater than the correlation length  $\xi$ . In networks, however, elastic neutron scattering measurements show "islands" of higher than average concentration and cross-link density, which

**Table IV**  
Relative Intensity of Static Scattering for Gel 1  
(Extrapolated)

$\theta$	$\lambda/\text{\AA}$	$Q/\text{\AA}^{-1}$	$I_S(Q)/[I_L(Q) + I_S(Q)]$
2.0	8.7	0.025	0.35
2.5	8.7	0.03	0.30
3.5	8.7	0.044	0.20
5.0	8.7	0.063	0.127
8.0	8.7	0.101	0.066
13.0	8.7	0.164	0.031
14.0	5.7	0.269	0.014
19.0	5.7	0.364	0.008

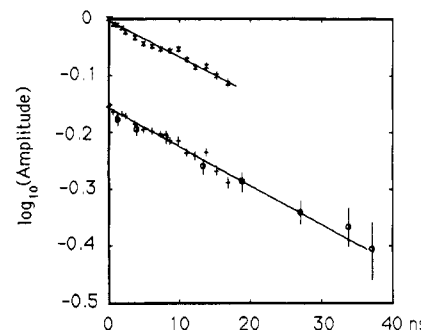


**Figure 7.** Neutron spin-echo decays at  $Q = 0.030$  Å<sup>-1</sup>. PDMS solution (\*) and swollen gel (+) at  $\lambda = 8.7$  Å,  $\theta = 2.5^\circ$ ; (O) gel at  $\lambda = 11.3$  Å,  $\theta = 3.2^\circ$ . The vertical shift between these decays is the correction for static scattering in the gel at this  $Q$ .

emerge when the gel is swollen. Such islands, although contributing strongly to the scattering signal,  $I_S$ , do not add significantly to the osmotic behavior of the whole gel.<sup>19</sup>

(2) **Macroscopic Impurities.** As described previously,<sup>22</sup> the present networks contain beads of a foreign polymer [poly(ethylsiloxane)] caused by precipitation of excess cross-linker. For the range of transfer wave vectors explored here, on account of the  $Q^{-4}$  dependence of this contribution, the static intensity  $I_{fp} = 2\pi S(d_{fp} - \bar{d})^2 Q^{-4}$  scattered by this source is negligibly small. (Here  $S$  is the internal surface of the beads,  $d_{fp}$  the scattering length density of the foreign polymer, and  $\bar{d}$  the mean scattering length density of the gel.)

The proportion in which the static component,  $I_S$ , contributes to the total scattering intensity depends upon the structure and distribution of the nonuniformities in concentration. Table IV lists the fraction of static scattering deduced from eqs 16 and 17 for the  $Q$  values explored in the spin-echo measurements. Figure 7 shows the spin-echo decays for the solution and the gel at  $\theta = 2.5^\circ$ ,  $\lambda = 8.7$  Å ( $Q = 0.030$  Å<sup>-1</sup>), after subtraction of this constant component from the gel signal. It is clear within experimental error that the echo from the solution decays at the same rate as that from the gel.

The above background subtraction procedure can be checked by extending the time delay in the echo. If the incident wavelength is increased to 11.3 Å, a relaxation time window of over 37 ns can be achieved. The result of this measurement for  $Q = 0.030$  Å<sup>-1</sup> is shown in Figure 7. The straight line is the least-squares fit through the data points below 20 ns; the coincidence between this fit and the data points at longer delay times indicates that the static base line is satisfactorily accounted for.

At the two lowest wave vectors explored,  $Q = 0.025$  and  $0.030$  Å<sup>-1</sup>, the data fit reasonably to straight lines in a semilogarithmic plot. At higher angles, deviations from single-exponential behavior arise, coming from the universal regime  $Q\xi > 1$ , where the initial decay rate  $\bar{\Gamma}$  varies

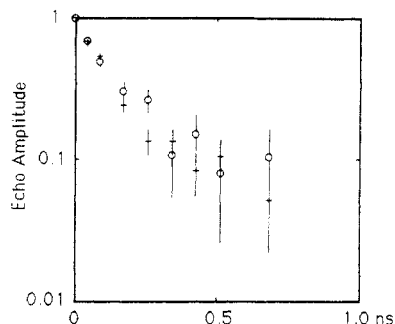


Figure 8. Corrected neutron spin-echo decays at  $Q = 0.364 \text{ \AA}^{-1}$ , for the solution (+) and for the gel (O), with an expanded time scale.

with  $Q$  as

$$\bar{\Gamma} \approx kTQ^3/6\pi\eta \quad (19)$$

Figure 8 displays the data points for the highest  $Q$  vector explored ( $Q = 0.365 \text{ \AA}^{-1}$ ), where it can be seen that the decays of the solution and gel are not distinguishable. In this regime, in order to compare the gel and the solution, it is sufficient for our purpose to analyze the data in terms of cumulant expansions. The results, shown in Figure 9, represent  $\bar{\Gamma}/Q^2$  for  $Q \geq 0.044 \text{ \AA}$ , where  $\bar{\Gamma}$  is the first cumulant in a two-cumulant fit to the data. Below this value of  $Q$  the data shown are obtained from a single-exponential fit. A remarkable feature of Figure 9 is the shortness of the range over which eq 19 applies: the range is in fact too short for the  $\bar{\Gamma}/Q^2 \propto Q$  (dashed line) to be properly attained.

**Quasi-Elastic Light Scattering.** The heterodyne correlation spectra from the solution gave good fits to single-exponential decays. For the gel, static scattering from the beadlike inclusions was intense, and the input aperture to the optics was stopped down so as not to overload the correlator. The corresponding decays were almost single exponential, displaying variances  $\mu_2/\bar{\Gamma}^2 \approx 0.05$ . The results of these measurements are plotted in Figure 9 at the left-hand ordinate axis. It can be seen that the datum for the solution coincides with that of the gel. Furthermore, the result of Munch et al.<sup>15</sup> for a PDMS solution at  $\varphi = 0.129$  (extrapolated to  $26^\circ\text{C}$ ), included in this figure as a vertical bar, is indistinguishable from the present solution and gel measurements. The present results are

$$\text{Gel: } \bar{\Gamma}/Q^2 = (1.5_1 \pm 0.1_7) \times 10^{-6} \text{ cm}^2 \text{ s}^{-1}$$

$$\text{Solution: } \bar{\Gamma}/Q^2 = (1.5_2 \pm 0.1_5) \times 10^{-6} \text{ cm}^2 \text{ s}^{-1}$$

$\bar{\Gamma}/Q^2$  can be related to the collective diffusion constant  $D_c$  by

$$\bar{\Gamma} = D_c Q^2 (1 - \varphi) \quad (20)$$

where the correction factor  $1 - \varphi$  results from the polymer displacement.<sup>42</sup> [More recently, Vink<sup>43</sup> has shown that when the symmetry of the kinetic coefficients is taken into account, the correction factor becomes  $(1 - \varphi)^2$ .] Thus

$$D_c = (1.7 \pm 0.2) \times 10^{-6} \text{ cm}^2 \text{ s}^{-1}$$

for both gel and solution at  $26^\circ\text{C}$ .

## Discussion

In Figure 9 it is clear that the present dynamic light scattering result for the PDMS solution is in agreement with that obtained by Munch et al.<sup>15</sup> by the same technique and also with the quasi-elastic neutron scattering mea-

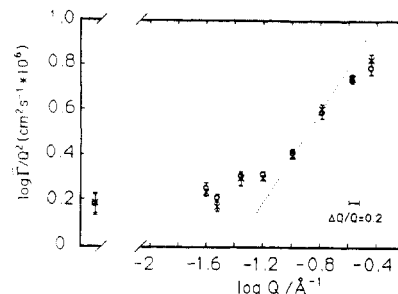


Figure 9. Corrected neutron spin-echo decay rates  $\bar{\Gamma}/Q^2$  from PDMS-toluene gel and solution, as a function of transfer wave vector  $Q$ : (O) gel; (X) solution. Data at the left-hand side of the diagram are QELS measurements on the same solution at  $Q = 6.4 \times 10^{-4} \text{ \AA}^{-1}$ ; the vertical bar is from Munch et al.,<sup>15</sup> corrected to  $26.5^\circ\text{C}$ . The slope of the dotted line is unity.

surement at the two lowest  $Q$  values. Because of the smaller number of time delay points in the spin-echo technique, the absolute uncertainty in  $\bar{\Gamma}/Q^2$  is larger than that in light scattering; the relative error with respect to the gel, however, is rather better. Furthermore, at higher  $Q$  values  $\bar{\Gamma}/Q^2$  for the gel and solution coincide within experimental error.

This result is interesting. In the intermediate  $Q$  range, the mobility of the polymer segments is proportional to  $Q/\eta$ , where  $1/Q$  is the radius of the segment investigated. The identity of  $\bar{\Gamma}$  in the solution and the gel in this  $Q$  range implies that the proportionality constant is the same in both cases. In the highest  $Q$  region explored, where a crossover to the motion of the single statistical units becomes visible, no significant difference can be seen either between the gel and the solution. This means that the difference in the osmotic properties between the gel and the solvent is not the result of differences in size of the statistical segments making up the polymer chains.

According to eqs 9a and 12, the ratio of the osmotic moduli in the gel and the solution,  $M_{os}/K_{os} \approx 1.10$ , will tend to make the ratio  $D_c^{\text{gel}}/D_c^{\text{sol}}$  greater than unity, a result which is observed in other gel systems.<sup>14-17</sup> In general, the diffusion coefficient can be expressed in the form<sup>44,45</sup>

$$D_c = \frac{kT}{6\pi\eta} \frac{\int_0^\infty S(Q)dQ}{S(0)}$$

In the present case, because of the presence of the precipitates, no information is available on the low  $Q$  behavior of the scattering function  $S(Q)$ .

In addition to the osmotic modulus, two other factors influence  $D_c$ .

First, cross-linking may affect the friction coefficient  $f$ . According to eq 2

$$f \propto \eta/\xi_{gH}^2$$

$\xi_{gH}$  being the hydrodynamic correlation length in the network. The NMR results of Table III favor a translational diffusion coefficient  $D_T$  of the solvent that is slightly higher in the gel than in the solution. Equation 18 can therefore be construed in terms of a lower solvent viscosity in the gel. It is known, however, that the solvent diffusion coefficient  $D_T$  in fluids containing slowly moving particles with volume fraction  $\varphi$  is reduced by a factor  $1 - \alpha\varphi$ , where  $\alpha = 3/2$  for spheres and  $\alpha = 5/3$  for rods.<sup>46,47</sup> This effect is an analogue of the Einstein viscosity correction for solid suspensions in a fluid.<sup>48</sup> Inspection of Table III reveals that the difference between  $D_T$  in the pure solvent and in solution agrees with  $\alpha = 5/3$ , i.e., the expectation for a

solution of linear polymers. Any reduction of  $\alpha$  on cross-linking may be attributed to the formation of branched clusterlike structures. This interpretation implies that the local solvent viscosity  $\eta$  is unaffected by structural changes.

Second, the differences in the concentration distribution between the solution and the gel, as observed by static neutron scattering, necessarily influence  $D_c$ . According to a model proposed previously for such gels,<sup>49</sup> the network concentration can be described by a Gaussian probability distribution about the average concentration  $\langle\varphi\rangle$  with a mean-square deviation  $\langle\delta\varphi^2\rangle$

$$\mathcal{P}(\varphi) = (2\pi\langle\delta\varphi^2\rangle)^{-1/2} \exp[-(\varphi - \langle\varphi\rangle)^2/2\langle\delta\varphi^2\rangle]$$

In such a gel, the intensity scattered by concentration fluctuations becomes

$$I(Q,t) = a \frac{\int_0^1 \mathcal{P}(\varphi) \frac{\varphi^2}{M_{os}} \exp(-D_c Q^2 t) d\varphi}{\int_0^1 \mathcal{P}(\varphi) d\varphi} \quad (21)$$

where  $a$  is an experimental proportionality constant. The first cumulant  $\bar{\Gamma}$  is obtained by expanding the exponent in the numerator of eq 21 at short times  $t$ :

$$\begin{aligned} \bar{\Gamma} &= - \left. \frac{d \ln [I(Q,t)]}{dt} \right|_{t=0} \\ &= \frac{\int_0^1 \mathcal{P}(\varphi) \frac{\varphi^2}{M_{os}} D_c Q^2 d\varphi}{\int_0^1 \mathcal{P}(\varphi) \frac{\varphi^2}{M_{os}} d\varphi} \end{aligned} \quad (22)$$

where the displacement term  $1 - \varphi$  in eq 20 is neglected. Introduction of scaling forms for  $M_{os} \propto \varphi^n$  and  $D_c \propto \varphi^s$  yields

$$\bar{\Gamma} = D_c(\langle\varphi\rangle) Q^2 \frac{\langle\varphi^{2+s-n}\rangle}{\langle\varphi^{2-n}\rangle} \quad (23)$$

where  $D_c(\langle\varphi\rangle)$  is the collective diffusion coefficient of an ideal uniform gel with mean concentration  $\langle\varphi\rangle$ , and  $\langle\varphi^n\rangle$  is the  $n$ th moment of the concentration distribution in the gel. Extending the integration limits to  $\pm\infty$  and making use of the properties of the moments of Gaussian distributions, namely, for  $\langle\delta\varphi^2\rangle/\langle\varphi\rangle^2$  small, then to first order

$$\bar{\Gamma} = D_c(\langle\varphi\rangle) Q^2 \left[ 1 - \frac{s}{2}(2n-3-s) \frac{\langle\delta\varphi^2\rangle}{\langle\varphi\rangle^2} \right] \quad (24)$$

The relaxation rate of the nonuniform gel is thus smaller than that of a uniform network of the same overall concentration  $\langle\varphi\rangle$ . For the PDMS gel investigated, the second moment of eq 18 gives

$$\begin{aligned} 2\pi^2(d_p - d_s)^2 \langle\delta\varphi^2\rangle &= M_2 \\ &= 1.45 \times 10^{20} \text{ cm}^{-4} \end{aligned}$$

From the neutron scattering densities of PDMS and toluene<sup>50</sup>

$$(d_p - d_s)^2 = 3.09 \times 10^{21} \text{ cm}^{-4}$$

yielding

$$\langle\delta\varphi^2\rangle = 2.4 \times 10^{-3}$$

and hence

$$\langle\delta\varphi^2\rangle/\langle\varphi\rangle^2 \approx 0.15$$

With  $n = 2.3$  and  $s = 0.75$ , eq 24 leads to a reduction in  $D_c$  of approximately 5% over a uniform gel of the same concentration.

The above discussion may be summarized by expressing the ratio of collective diffusion coefficients in the gel (g) and the solution (s) as

$$\frac{D_c^g}{D_c^s} = \left( \frac{M_{os}}{K_{os}} \right) \left( \frac{\xi_{gH}}{\xi_{sH}} \right)^2 \left[ 1 - \frac{s}{2}(2n-3-s) \frac{\langle\delta\varphi^2\rangle}{\langle\varphi\rangle^2} \right] \quad (25)$$

Equation 25 shows that the relation between  $D_c$  in the gel and solution is the result of different competing effects.  $M_{os}$  is expected to be greater than  $K_{os}$ , on account of the finite shear modulus ( $M_{os} = K_{os} + 4G/3$ ). The last factor in eq 25 depends strongly on the structure of the particular network and hence on the details of cross-linking: increasing the nonuniformity of the network, i.e.,  $\langle\delta\varphi^2\rangle/\langle\varphi\rangle^2$ , causes a reduction in the observed value of the relaxation rate in the gel. In an inhomogeneous network, the meaning of the correlation length is no longer well-defined, the apparent value measured in a scattering experiment being determined by the concentration, cross-linking density, and chemical composition, which can vary strongly from one region to another in the gel. Because of these competing effects, it is hardly reasonable to expect simple proportionality to hold between the hydrodynamic and the static correlation lengths,  $\xi_H$  and  $\xi_s$ . Equation 25 provides an explanation of the apparently conflicting observations of the ratio of the cooperative diffusion coefficient in the gel and in the corresponding polymer solution. Since the right-hand side of eq 25 is governed by several factors acting in opposing directions, for different gels  $D_c^g$  may be smaller than, equal to, or greater than  $D_c^s$ .

## Conclusions

Combined measurements by elastic and quasi-elastic neutron scattering, quasi-elastic light scattering, nuclear magnetic resonance, and swelling pressure on a PDMS gel swollen in toluene and the equivalent solution give a converging picture of various competing effects that operate in the swollen network.

As has been found for other concentrated gel systems, nonuniformities in the network concentration play a major role in the average response of the system. For the gel investigated here, the solvent mobility is marginally increased by cross-linking, because of the formation of branched aggregates. The osmotic component of the longitudinal modulus  $M_{os}$  governing the scattering intensity is appreciably depressed. No structural changes in the statistical units are detected by the neutron spin-echo measurements. All the discrepancies observed between the present gel and the solution appear to be the consequence of the nonuniformities of the network.

**Acknowledgment.** We are grateful to P. Pruvost of Rhône-Poulenc (Département Silicones) for supplying the samples. The neutron scattering experiments were performed at the Institut Laue-Langevin, Grenoble, France. This work is part of an agreement between the Centre National de Recherche Scientifique (CNRS) and the Hungarian Academy of Sciences and is supported by Grant OTKA No. 2158. The experiments were performed during the tenure of a Visiting Professorship of F.H. at the Université Joseph Fourier de Grenoble.



## References and Notes

- (1) Flory, P. J.; Rehner, J., Jr. *J. Chem. Phys.* **1943**, *11*, 521.
- (2) Flory, P. J. *Principles of Polymer Chemistry*; Cornell University Press: Ithaca, NY, 1953.
- (3) de Gennes, P.-G. *Scaling Concepts in Polymer Physics*; Cornell University Press: Ithaca, NY, 1979.
- (4) Gee, G.; Herbert, J. B.; Roberts, R. C. *Polymer* **1965**, *6*, 541.
- (5) Yen, L. Y.; Eichinger, B. E. *J. Polym. Sci., Polym. Phys. Ed.* **1978**, *16*, 121.
- (6) Brotzman, R. W.; Eichinger, B. E. *Macromolecules* **1981**, *14*, 1445; **1982**, *15*, 531; **1983**, *16*, 1131.
- (7) Neuburger, N. A.; Eichinger, B. E. *Macromolecules* **1988**, *21*, 3060.
- (8) Langley, N. R.; Ferry, J. D. *Macromolecules* **1968**, *1*, 353.
- (9) McKenna, G. B.; Flynn, K. M.; Chen, Y. *Polym. Commun.* **1988**, *29*, 272.
- (10) Freed, K. F.; Pesci, A. I. *Macromolecules* **1989**, *22*, 4048.
- (11) Geissler, E.; Horkay, F.; Hecht, A.-M.; Zrinyi, M. *J. Chem. Phys.* **1989**, *90*, 1924.
- (12) Horkay, F.; Hecht, A.-M.; Geissler, E. *J. Chem. Phys.* **1989**, *91*, 2706.
- (13) Tanaka, T.; Hocker, L. O.; Benedek, G. B. *J. Chem. Phys.* **1973**, *59*, 5151.
- (14) McAdam, J. D. G.; King, T. A.; Knox, A. *Chem. Phys. Lett.* **1974**, *26*, 64.
- (15) Munch, J. P.; Lemaréchal, P.; Candau, S.; Herz, J. *J. Phys. (Les Ulis, Fr.)* **1977**, *38*, 1499.
- (16) Bastide, J.; Duplessix, R.; Picot, C.; Candau, S. *Macromolecules* **1984**, *17*, 83.
- (17) Sellen, D. B. *J. Polym. Sci., Part B: Polym. Phys.* **1987**, *25*, 699.
- (18) Fang, L.; Brown, W. *Macromolecules* **1990**, *23*, 3284.
- (19) Mallam, S.; Horkay, F.; Hecht, A. M.; Rennie, A. R.; Geissler, E. *Macromolecules* **1991**, *24*, 543.
- (20) Horkay, F.; Hecht, A.-M.; Mallam, S.; Geissler, E.; Rennie, A. R. *Macromolecules* **1991**, *24*, 2896.
- (21) Hecht, A.-M.; Horkay, F.; Geissler, E.; Benoit, J. P. *Macromolecules* **1991**, *24*, 4183.
- (22) Mallam, S.; Hecht, A.-M.; Geissler, E.; Pruvost, P. *J. Chem. Phys.* **1989**, *91*, 6447.
- (23) Geissler, E.; Horkay, F.; Hecht, A.-M. *Macromolecules* **1991**, *24*, 6006.
- (24) Horkay, F.; Zrinyi, M.; Geissler, E.; Hecht, A.-M.; Pruvost, P. *Polymer* **1991**, *32*, 835.
- (25) Vink, H. *Eur. Polym. J.* **1974**, *10*, 149.
- (26) Nagy, M.; Horkay, F. *Acta Chim. Acad. Sci. Hung.* **1980**, *104*, 49.
- (27) Shih, H.; Flory, P. J. *Macromolecules* **1972**, *5*, 761.
- (28) Stejskal, E. O.; Tanner, J. E. *J. Chem. Phys.* **1965**, *42*, 288.
- (29) Callaghan, P. T.; Trotter, C. M.; Jolley, K. W. *J. Magn. Reson.* **1980**, *37*, 247.
- (30) Vrentas, J. S.; Duda, J. L.; Ling, H. C.; Hou, A. C. *J. Polym. Sci., Polym. Phys. Ed.* **1985**, *23*, 289.
- (31) Mezei, F. *Z. Phys.* **1972**, *255*, 146.
- (32) Richter, D.; Hayter, J. B.; Mezei, F.; Ewen, B. *Phys. Rev. Lett.* **1978**, *41*, 1484.
- (33) Nicholson, L. K.; Higgins, J. S.; Hayter, J. B. In *Proc. International Workshop on Neutron Spin Echo*; Mezei, F., Ed.; Springer Lecture Note Series 128; Springer: Berlin, 1980.
- (34) Treloar, L. R. G. *The Physics of Rubber Elasticity*, 3rd ed.; Clarendon Press: Oxford, U.K., 1975.
- (35) Soni, V. K.; Stein, R. S. *Macromolecules* **1990**, *23*, 5257.
- (36) Porod, G. In *Small Angle X-ray Scattering*; Glatter, O., Kratky, O., Eds.; Academic Press: London, 1982.
- (37) Hecht, A.-M.; Duplessix, R.; Geissler, E. *Macromolecules* **1985**, *18*, 2167.
- (38) Bastide, J.; Leibler, L. *Macromolecules* **1988**, *21*, 2647.
- (39) Bastide, J.; Leibler, L.; Prost, J. *Macromolecules* **1990**, *23*, 1821.
- (40) de Gennes, P.-G. *J. Phys. (Les Ulis, Fr.)* **1981**, *42*, 735.
- (41) Richter, D.; Farago, B.; Fetters, L. J.; Huang, J. S.; Ewen, B.; Lartigue, C. *Phys. Rev. Lett.* **1990**, *64*, 1389.
- (42) Geissler, E.; Hecht, A.-M. *J. Phys. Lett. (Les Ulis, Fr.)* **1979**, *40*, L-173.
- (43) Vink, H. *J. Chem. Soc., Faraday Trans. 1* **1985**, *81*, 1725.
- (44) Kubo, R. *J. Phys. Soc. Jpn.* **1957**, *12*, 570.
- (45) Schosseler, F.; Moussaid, A.; Munch, J. P.; Candau, S. *J. J. Phys. II (Fr.)* **1991**, *1*, 1197.
- (46) Wang, J. H. *J. Am. Chem. Soc.* **1954**, *76*, 4755.
- (47) Johansson, L.; Elvingson, C.; Löfroth, J.-E. *Macromolecules* **1991**, *24*, 6024 and references therein.
- (48) Landau, L. D.; Lifshitz, E. M. *Fluid Mechanics*; Pergamon Press: Oxford, U.K., 1959.
- (49) Geissler, E.; Hecht, A. M.; Horkay, F.; Zrinyi, M. *Macromolecules* **1988**, *21*, 2594.
- (50) Lovesey, S. W. *Theory of Neutron Scattering from Condensed Matter*; Clarendon Press: Oxford, U.K., 1984.